SLAC-PUB-1965
U.C.S.C. 76-063
June 1977
(T/E)

STRUCTURE FUNCTIONS AND CHARGE RATIOS IN MUON NUCLEON SCATTERING*

C. del Papa,[†] D. Dorfan, S.M. Flatté, C.A. Heusch
B. Lieberman,[††] H. Meyer,[†††] L. Moss, T. Schalk, A. Seiden

University of California
Santa Cruz, California

and

K. Bunnell, M. Duong-van, R. Mozley, A. Odian, F. Villa, L.C. Wang

Stanford Linear Accelerator Center
Stanford, California

Abstract

We present the fractional energy distributions for positive and negative hadrons produced in muon-proton and muon-neutron scattering, and ensuing charge ratios for the photon fragmentation region. Data presented for a center-of-mass energy range $2.8 < W < 4.7$ GeV and a virtual-photon mass-squared range $.5 \leq Q^2 \leq 4.5$ GeV^2 indicate an overall equality of summed structure functions for neutron and proton targets, which exhibit approximate independence of Q^2 and ω'. Implications in terms of quark fragmentation ideas are discussed.

---

*Supported in part by the Energy Research and Development Administration.

[†]Now at CERN, Geneva, Switzerland

[††]Now at ETEC Corporation, Hayward, California

[†††]Now at the University of Wuppertal, Germany

(Submitted to Phys. Rev. Letters)

I. Introduction

The scattering of a muon on a nucleon target occurs to lowest order via the exchange of a virtual photon. Leading contenders for the physics interpretation of the observed phenomena are diffractive models or a parton scattering picture[1]. In this Letter, we explore features of the hadronic final-states for both proton and neutron targets, concentrating on the individual particle energy distributions (or "structure functions"). We demonstrate that the distributions from neutron and proton targets are independent of the scaling variable ω' and the virtual-photon mass squared Q^2. While there are marked differences between the individual charge states, the energy distribution of charged particles from neutrons, summed over positives and negatives, is remarkably similar to the distribution from protons. We interpret these regularities in terms of the parton contents of the nucleons.

Each event can be characterized by the quantity Q^2, and the center-of-mass energy, W, of the virtual photon-nucleon system. These together make up the scaling variable $\omega' = 1 + \frac{W^2}{Q^2}$. The structure of the final states produced in these events can be analyzed in terms of the density of particles materializing in the "fragmentation" region of the incoming virtual photon. This density can be parametrized by the fraction of the incoming energy, $z = E_h/\nu$, carried by each hadron in the laboratory reference frame[2]. This variable is a Lorentz invariant quantity $p\cdot h/p\cdot q$, where p_α, h_α, q_α are the initial-nucleon, final-hadron, and virtual-photon 4-momenta. The distribution function for hadrons of type h and a target of type N (= p or n),

$$F_{\mu N}^{(h)} = \frac{1}{\sigma_{tot}} \; z \frac{d\sigma_N^{(h)}}{dz} ,$$

is often called a hadronic "structure function." $\sigma_N^{(h)}$ is the inclusive

cross section for production of hadrons of type h off target nucleon N. We present results on these functions for positive and negative hadrons produced from proton and neutron targets. Comparisons for different lepton probes can be found in Ref. 2. The experiments, performed in the two-meter-long SLAC streamer chamber, are described in Ref. 3 and 4. The results for the neutron were obtained using a deuterium target, after a subtraction of the proton component. The details of the subtraction are described in Ref. 4; all error bars for the neutron case take into account the errors coming from this procedure. To improve our statistical samples, we also show some results summed over target types; for these we add both the hydrogen and the deuterium data. We note here: that low momentum tracks are lost in an inactive region of the chamber; that there is a contamination of spectator protons at low momentum from the deuterium target, and that there is no particle identification. Therefore, we ignore hadrons below z of .1, leaving predominantly pions, with a small admixture of kaons and protons.

II. Structure Functions

In Fig. 1, we display the structure functions $F_{\mu p}^{(h^+)}$, $F_{\mu p}^{(h^-)}$, $F_{\mu n}^{(h^+)}$, and $F_{\mu n}^{(h^-)}$ as a function of z, for three bins in ω'. In calculating E_h, all particles are assumed to be pions. The average Q^2 for the ω' bins chosen is 0.6, 1.0, and 2.3 GeV^2. Over this range, the structure functions show little dependence on ω'. Therefore, we sum over the three ω' bins and compare the four resulting structure functions directly in Fig. 2. All four functions appear to follow different trends at essentially all z values; also, the functions for h^+ are noticeably larger than those for h^-, for both proton and neutron targets.

We can now combine all final-state charged particles, to form the functions

$$F_{\mu p} = F_{\mu p}^{(h^+)} + F_{\mu p}^{(h^-)} \text{ and } F_{\mu n} = F_{\mu n}^{(h^+)} + F_{\mu n}^{(h^-)} .$$

They are shown in Fig. 3 for data summed over all three ω' bins. Although the four components making up these two functions differ in magnitude and trend, as seen in Fig. 2, the summed functions $F_{\mu p}$ and $F_{\mu n}$ are seen to be approximately equal to each other.

III. Charge Ratio

We now study the charge differences seen in the structure functions in Fig. 2, by calculating the ratio:

$$R_N(\omega') = \frac{\int_{.3}^{1.} F_{\mu N}^{(h^+)}(z)\, dz}{\int_{.3}^{1} F_{\mu N}^{(h^-)}(z)\, dz} .$$

This ratio is the fraction of the incoming energy carried by positive particles with $z \geq .3$ divided by a similar fraction for negative particles. (Note that about 1/3 of the available energy is carried by charged particles with $z \geq .3$.) This z range comprises the so-called fragmentation region of the virtual-photon.

Values of $R_p(\omega')$ and $R_n(\omega')$ are shown in Fig. 4 for the three ω' bins used earlier. $R_p(\omega')$ and $R_n(\omega')$ are comparable in value for $\omega' \geq 9$. All values are greater than 1., indicating that positives carry more of the available energy than negatives in the photon fragmentation region. Similar results for the particle multiplicity in this region can be found in Refs. 5, 6, and 7. These results will be discussed further in the next section.

IV. Test of the Quark-Parton Model

The quark parton model provides some unique constraints on the values of the structure functions for large z. Assuming that

(1) we can ignore the presense of strange quarks in the proton,

(2) the final-state particles are nearly all pions,

we can write the four structure functions as follows[2]:

$$F_{\mu N}^{(h^+)} = z\left[P_u^N(\omega')\, D_u^{\pi^+}(z) + \left(1 - P_u^N(\omega')\right) D_u^{\pi^-}(z)\right]$$

$$F_{\mu N}^{(h^-)} = z\left[P_u^N(\omega')\, D_u^{\pi^-}(z) + \left(1 - P_u^N(\omega')\right) D_u^{\pi^+}(z)\right]$$

where N = proton or neutron, and $P_u^N(\omega')$ is the probability that the quark, which is scattered by the virtual photon, is u or $\bar{d}$. (These two are linked by isospin and C invariance.) $D_u^{\pi^+}(z)$ and $D_u^{\pi^-}(z)$ are the fragmentation functions of a u (or $\bar{d}$) into π^+ and π^-, respectively. These ideas have been tested, using models for $P_u^N(\omega')$, for example, in Ref. 5. Our results in Fig. 4 could provide a similar check. However, we wish to check the fragmentation ideas without taking recourse to any assumptions about $P_u^N(\omega')$. For this purpose we sum over h^+ and h^- and get:

$$F_{\mu p} = z\left(D_u^{\pi^+}(z) + D_u^{\pi^-}(z)\right)$$

$$F_{\mu n} = z\left(D_u^{\pi^+}(z) + D_u^{\pi^-}(z)\right) .$$

Thus, the quark-parton model predicts that:

(1) $F_{\mu p} = F_{\mu n}$.

(2) Both of these should show <u>no</u> Q^2 or ω' dependence.

The presence of final state particles other than pions occurs at about the 25% level[6,7]. However, the data of references (6) and (7) show that the ratio of kaons and protons to pions is independent of ω', Q^2, and target type, to the level of less than 10% of the pions, so that the above predictions are not significantly effected by kaon and proton contamination in the photon fragmentation region.

The first of these results, $F_{\mu p} = F_{\mu n}$, was borne out approximately in Fig. 3. To check the second prediction with maximum sensitivity, we add together all data obtained in the proton and deuterium experiments for each of the three ω' bins separately, and display the resulting z distributions in Fig. 5. A universal function, showing little or no ω' (or Q^2) dependence results, as predicted. For $z > 0.20$, it is well represented by a single exponential.

If we interpret the observed charge ratios in terms of the quark-parton model, we must consider both the valence and sea quarks in the nucleon. In this framework, the charge ratios greater than 1 imply that scattering of valence quarks is important even at large ω' ($\sim$30), since the sea would give a unit ratio for both proton and neutron targets. This is expected from typical estimates for the quark content of the nucleon[8] based on the total inelastic cross section only. The near equality of the charge ratios for protons and neutrons at large ω' values, $\gtrsim 9$, would then require a similar valence content in this region, as also indicated by the data in Ref. 7. This requires that one valence quark (u for the proton, d for the neutron) be unlikely to be found at large ω', leaving, for both target types, a ud diquark structure at these ω' values. A single quark would then be expected to dominate the scattering at small ω', leading to a neutron-to-proton cross section ratio of ¼. A small value for this ratio has long been established experimentally[9].

A model which populates the photon fragmentation region with diffractive vector meson production only, would be hard to reconcile with the data since it would predict no dependence on target type or charge state of the produced hadrons. However, there is a significant contribution from elastic ρ^0 production at very large z[2].

References

1. R.P. Feynman, Photon-Hadron Interactions (W.A. Benjamin, Reading, MA, 1972).
   M. Gronau, F. Ravndal, and Y. Zarmi, Nucl. Phys. B51, 611 (1973).

2. C. del Papa et al., Phys. Rev. D15, 2425 (1977).

3. C. del Papa et al., Phys. Rev. D13, 2934 (1976).

4. C. del Papa et al., U.C.S.C. preprint #76-052.

5. J. T. Dakin and G.J. Feldman, Phys. Rev. D8, 2862 (1973).

6. K. Hanson, talk presented at the 1975 International Symposium on Lepton and Photon Interactions at High Energies, Stanford, California.

7. J.F. Martin et al., Phys. Lett. 65B, 483 (1976).
   J.F. Martin and L.S. Osborne, Phys Rev. Lett. 38, 1193 (1977).

8. T. Kuti and V.F. Weisskopf, Phys. Rev. D4, 3418 (1971).
   R. McElhaney and S.F. Tuan, Phys. Rev. D8, 2267 (1973).
   J.F. Gunion, Phys. Rev. D10, 242 (1974).
   M. Duong-van, Phys. Lett. 60B, 287 (1976).

9. A. Bodek et al., Phys. Rev. D7, 1362 (1973).

Figure Captions

1. The structure functions for positive and negative hadrons produced at $z > .1$ from proton and neutron targets in three bands of ω'. The average ω' values for the three bands are 6.5, 14, and 27. The bin widths are .1 below, and .2 above $z = .4$. Some data points are displaced from the bin centers for visibility.

2. Hadron structure functions integrated over ω', with bin widths of .1 for $.1 < z < .2$, and .2 for $z > .2$. Some data points are displaced from bin centers for visibility.

3. The hadron structure function integrated over ω' and summed over both charge states, with bin widths of .1. Some data points are displaced from bin centers for visibility.

4. The charge ratios for $z > .3$ from proton and neutron targets.

5. The structure function for charged hadrons produced at $z > .1$ from a nucleon target in three bands of ω'. Data from proton and deuteron targets, and for positive and negative hadrons, are summed. Some data points are displaced from the centers of the bins (of width .1) for visibility. In order to conveniently parameterize the data, we performed a least-squares fit to the form Ae^{-Bz}. The resulting curve, shown in the figure, had a χ^2 of 22.2 for 22 degrees of freedom; the parameters are $A = 2.22 \pm .07$ and $B = 2.62 \pm .08$.

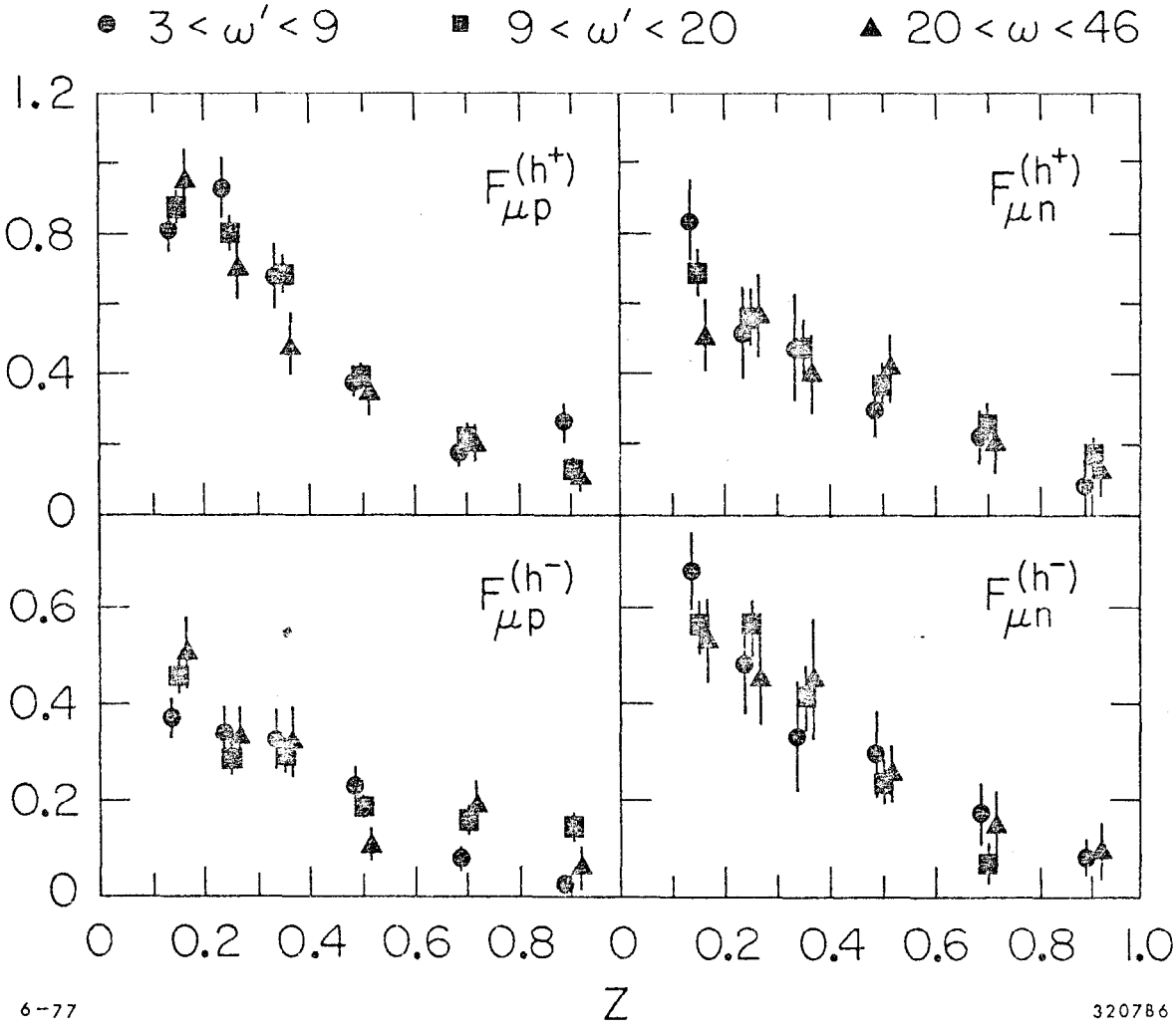
3 < ω′ < 9
9 < ω′ < 20
20 < ω < 46
$F_{\mu p}^{(h^+)}$
$F_{\mu n}^{(h^+)}$
$F_{\mu p}^{(h^-)}$
$F_{\mu n}^{(h^-)}$
1.2
0.8
0.4
0
0.6
0.4
0.2
0
0
0.2
0.4
0.6
0.8
0
0.2
0.4
0.6
0.8
1.0
Z
6-77
3207B6

Fig 1

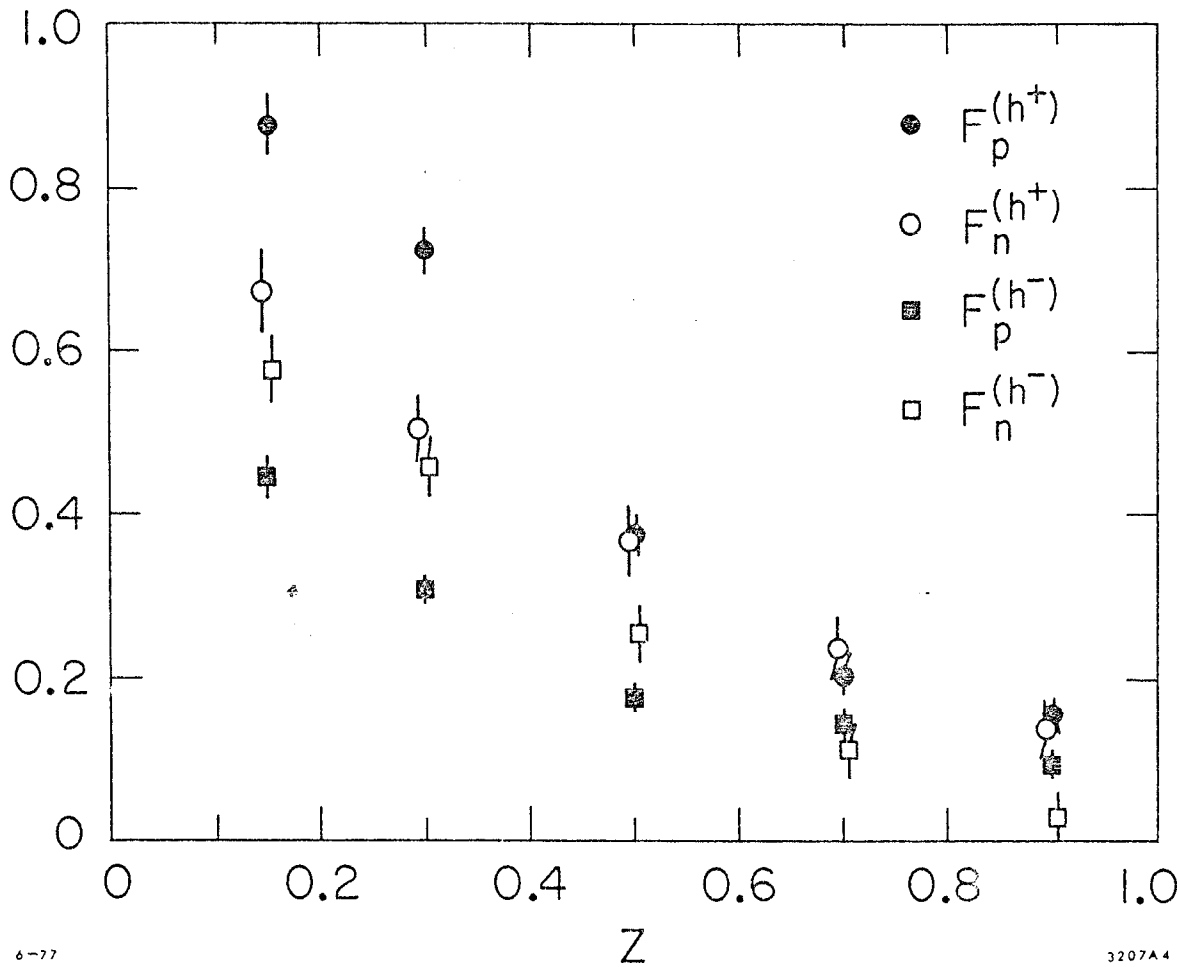

Fig. 2

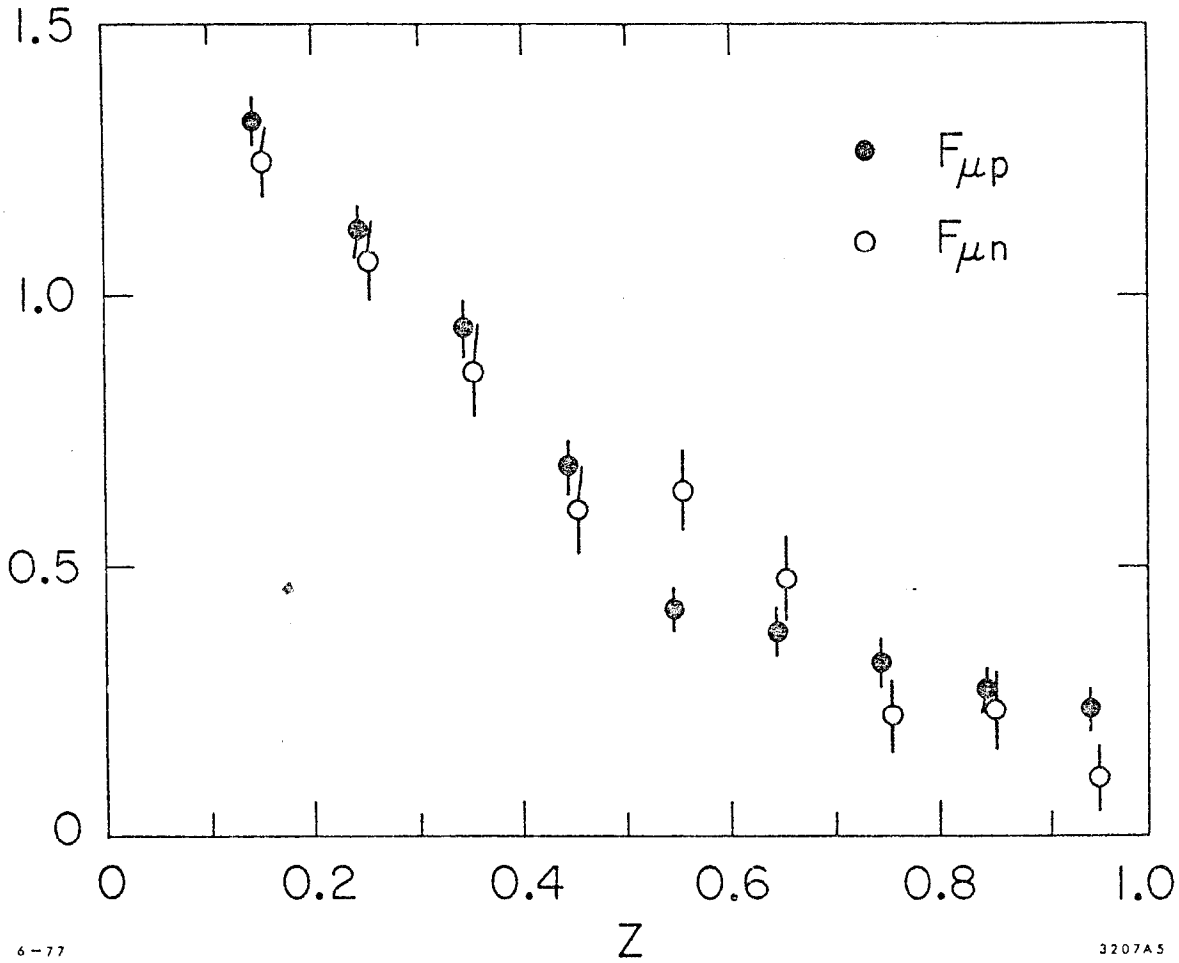

Fig. 3

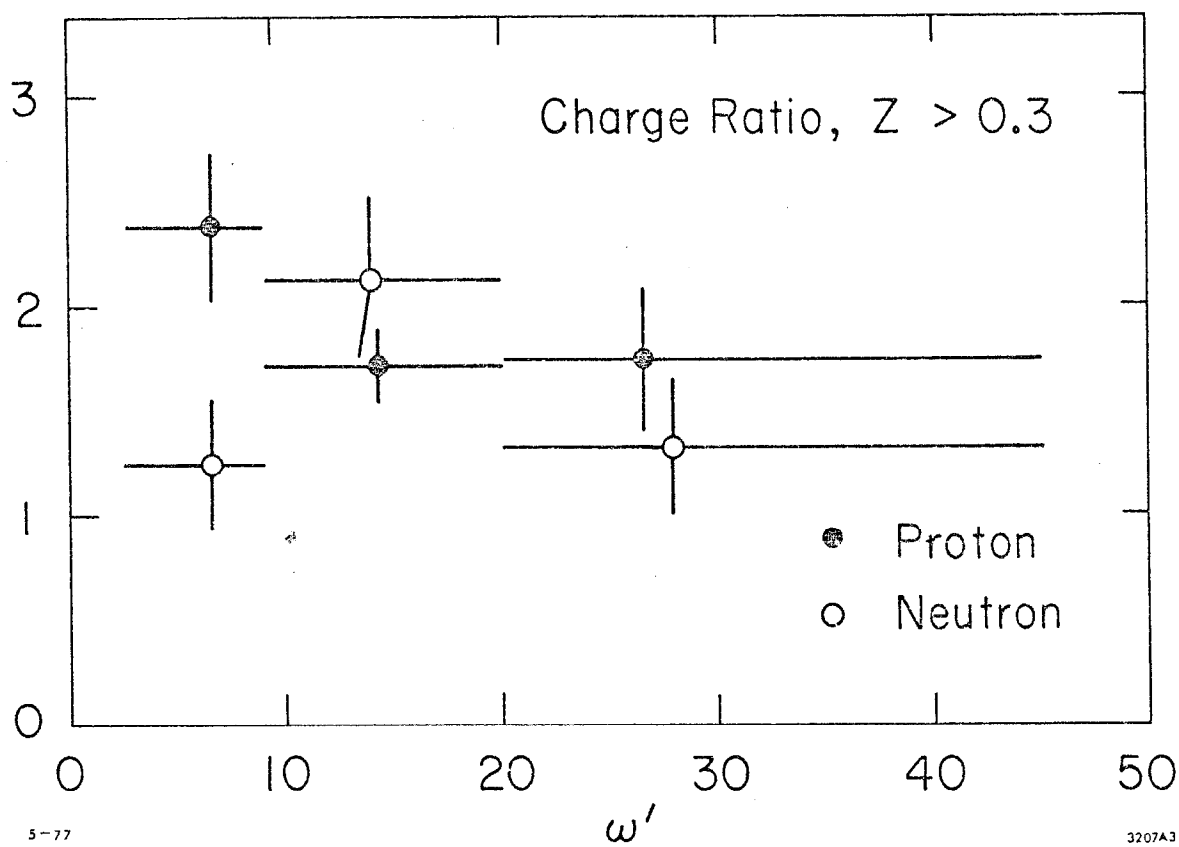
Charge Ratio, Z > 0.3
Proton
Neutron
0
1
2
3
0
10
20
30
40
50
ω′
5-77
3207A3

Fig. 4

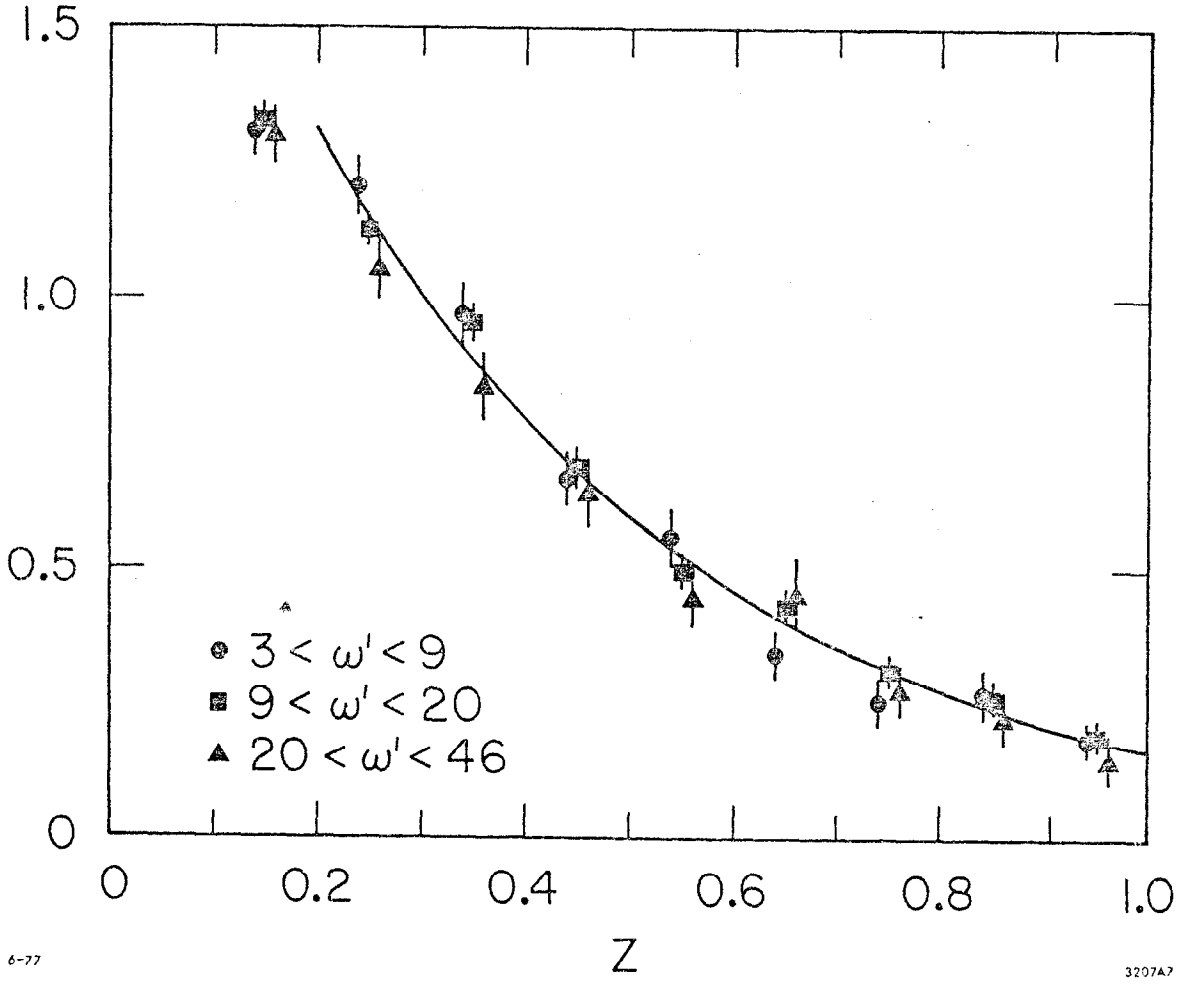

Fig. 5